

Deflection of jets induced by jet-cloud & jet-galaxy interactions

S. Mendoza & M.S. Longair

Cavendish Laboratory, Madingley Rd., Cambridge CB3 0HE, U.K.

28 October 2018

ABSTRACT

The model first introduced by Raga & Cantó (1996) in which astrophysical jets are deflected on passing through an isothermal high density region is generalised by taking into account gravitational effects on the motion of the jet as it crosses the high density cloud. The problem is also generalised for relativistic jets in which gravitational effects induced by the cloud are neglected. Two further cases, classical and relativistic, are discussed for the cases in which the jet is deflected on passing through the interstellar gas of a galaxy in which a dark matter halo dominates the gravitational potential. The criteria for the stability of jets due to the formation of internal shocks are discussed.

Key words: Hydrodynamics – Relativity – Galaxies: Active – Galaxies: Jets

1 INTRODUCTION

According to the standard model for Fanaroff-Riley type II radio sources, a pair of relativistic jets of electrons is ejected in opposite directions from a very compact region in the nucleus of an elliptical galaxy (Blandford 1990). The jets expand adiabatically through the interstellar medium of the host galaxy and the surrounding intergalactic medium. Collimation of the jets is provided by the presence of a cavity or “cocoon” surrounding the jet, which maintains the pressure of the intergalactic medium in balance with that of the relativistic gas within the jet. In this model, the jets maintain a straight trajectory. However, observations have shown that jets often bent.

Dramatic changes in morphology are found in radio trails sources (for example NGC 1265), in which the jets have a semicircular shape, with the host galaxy at the pole. The curvature of the jet is attributed to the motion of the host galaxy through the intracluster medium which results in a significant ram pressure acting on the jet (Begelman, Blandford & Rees 1984).

Some deflections may result from a combination of kinetic and geometrical effects. For example, the precession of jets about a defined axis can cause the jet to be curved, although any fluid element in the jet always follows a straight trajectory. Another example is the proper motion of a galaxy through the intergalactic medium produced by the gravitational influence of a companion galaxy (Begelman, Blandford & Rees 1984). Again, each fluid element in the jet follows a straight trajectory. However, since the galaxy producing the jet moves in an orbit about its companion, the jet appears to be curved.

Another way of inducing deflections in radio jets is if the

beam passes through a region of interstellar or intergalactic gas in which there is a significant pressure gradient. This might occur if the jets pass through the interstellar medium of a large galaxy or diffuse intergalactic cloud. There are a few cases in which this may have occurred. In the case of 3C34 Best, Longair & Röttgering (1997) found evidence that the jet had interacted strongly with the interstellar medium of a galaxy which happened to lie in the path of the jet. More evidence for misalignments between one of the hotspots of a radio galaxy and the host galaxy was found in 3C324 and 3C368 (Best et al. 1998). In these objects, no galaxy has been found in the path of the jets, but there is strong evidence for the presence of high density regions from the optical and infrared observations. For sources in which the jet has given rise to optically aligned emission regions, the optical emission is most probably produced by shock emission (Best, Röttgering and Longair 2000). The present study was motivated by these observations, the objective being to find a simple prescription for how significant the deflections of the radio jets could be if they passed through the interstellar medium of an intervening galaxy or gas cloud. In addition, we have analysed the stability of these deflections against to the formation of internal shocks. This stability analysis will be published elsewhere, but we discuss the results at the end of this article.

The work presented here is an extension of the model first proposed by Cantó & Raga (1996) and Raga & Cantó (1996) in order to describe how deflections of radio jets are produced in jet/cloud interactions. The steady interaction of a jet with an isothermal sphere is analysed in two ways. Firstly we describe the steady interaction of a classical jet (i.e. a jet for which its internal velocities and thermal effects are not relativistic) with an isothermal cloud in which the

arXiv:astro-ph/0008015v3 31 Mar 2001

self gravity of the cloud is taken into account. This is similar to the analysis of Raga & Cantó (1996), but generalised in order to take into account the effects of gravity. We also analyse the steady interaction of a relativistic jet with an isothermal sphere in which the gravity of the cloud is not taken into account. In this case, it is possible to integrate the relevant equations exactly. Secondly, we consider a more relevant case for galaxies, in which it is assumed that all the gas in the galaxy is in hydrostatic equilibrium within a dark matter halo. Again, the cases of classical and relativistic jets are discussed.

2 JET/CLOUD INTERACTIONS

The interaction of an astrophysical jet with a cloud, in which the characteristic size of the cloud is much greater than the jet radius, has been studied in its initial stages by Raga & Cantó (1995). They showed that initially the jet slowly begins to bore a passage into the cloud. Eventually a stationary situation is achieved in which the jet penetrates the cloud and escapes from it in a direction which is different from the original jet trajectory.

Once the steady state is reached, the trajectory is determined by maintaining pressure equilibrium with the surrounding environment. In other words, as the material in the jet moves, it adjusts its pressure in such a way that it is in equilibrium with the internal pressure of the cloud. Since the expansion of the jet is adiabatic, and a steady state has been reached, Bernoulli's equation can be used to describe the trajectory of the jet as it passes through the cloud. In what follows the interaction of a jet with a cloud of characteristic radius much greater than the diameter of an adiabatic jet is analysed, once the steady state configuration has been reached.

3 CLASSICAL ANALYSIS

In the classical case, the motion of a fluid element in the jet is determined by Euler's equation:

$$\frac{\partial \mathbf{v}}{\partial t} + \mathbf{v} \cdot \mathbf{grad} \mathbf{v} = -\frac{1}{\rho} \mathbf{grad} p - \mathbf{grad} \phi, \quad (1)$$

where \mathbf{v} is the velocity of the flow, and p and ρ are pressure and density. The gravitational force produced by the cloud is described in the term which contains the gravitational potential ϕ . The left hand side of eq.(1) is the force per unit mass experienced by a fluid element as it moves. Since all quantities depend only on the distance from the cloud's centre \mathbf{r} , vector multiplication of the radius vector \mathbf{r} with eq.(1) implies $\mathbf{r} \times d\mathbf{v}/dt = 0$. In other words, the specific angular momentum $\mathbf{l} = \mathbf{r} \times \mathbf{v}$ is conserved as the fluid moves. Since the radius vector is perpendicular to the angular momentum vector, the motion is two dimensional, and so, polar coordinates (r, φ) are used in the following analysis.

Consider a situation in which the jet enters the cloud parallel to the x axis at a distance r_0 , so that its velocity vector is initially given by:

$$\mathbf{v}_0 = -v_0 \mathbf{e}_x = -v_0 (\cos \varphi_0 \mathbf{e}_r - \sin \varphi_0 \mathbf{e}_\varphi), \quad (2)$$

where \mathbf{e}_x , \mathbf{e}_r and \mathbf{e}_φ are unit vectors in the directions x , r and φ respectively. Because angular momentum is conserved and the motion is two dimensional, the velocity is most simply written using eq.(2) as:

$$\mathbf{v} = v_r \mathbf{e}_r + \frac{r_0}{r} v_0 \sin \varphi_0 \mathbf{e}_\varphi, \quad (3)$$

in which $v_r = dr/dt$ represents the velocity in the radial direction.

Since the steady flow of inside the jet expands adiabatically, we can calculate its path of by means of Bernoulli's equation:

$$\frac{1}{2} \int dv^2 + \int dw + \int d\phi = 0, \quad (4)$$

in which the line integrals are taken from the initial position of a given fluid element to its final one. The enthalpy per unit mass w of the flow in the jet is given by $w = \Gamma^{-1} p / \rho$ and $\Gamma \equiv (\gamma - 1) / \gamma$ for a gas with polytropic index γ .

Substituting eq.(3) and eq.(2) into the first integral of eq.(4) gives:

$$\int dv^2 = \left\{ \frac{r_0}{r} \frac{v_0 \sin \varphi_0}{r} \frac{dr}{d\varphi} \right\}^2 + v_0^2 \left\{ \left(\frac{r_0}{r} \right)^2 \sin^2 \varphi_0 - 1 \right\}, \quad (5)$$

where we have used the fact that along the jet trajectory $dr/v_r = r d\varphi/v_\varphi$. Since the gas in the jet obeys a polytropic equation of state, we obtain for the second integral in eq.(4):

$$\int dw = \frac{c_0^2}{\gamma \Gamma} \left\{ \left(\frac{p}{p_0} \right)^\Gamma - 1 \right\}, \quad (6)$$

in which c_0^2 is the initial sound speed of the jet material. The integral for the gravitational potential produced by the self-gravitating cloud is obtained from:

$$\int d\phi = G \int \frac{M(r)}{r^2} dr = 4\pi G \int \frac{dr}{r^2} \int_0^r \xi^2 \rho_c(\xi) d\xi, \quad (7)$$

where $M(r)$ and $\rho_c(r)$ represent the mass and density of the cloud at a distance r . Substitution of eqs.(5)-(7) into eq.(4) gives the equation for the path of the jet as it expands:

$$\frac{d\eta}{d\varphi} = \pm \frac{1}{\sin \varphi_0} \left\{ 1 - \eta^2 \sin^2 \varphi_0 - \frac{2}{\gamma \Gamma M_0^2} \times \left[\left(\frac{p}{p_0} \right)^\Gamma - 1 \right] - \frac{8\pi G}{M_0^2 c_0^2} \int \frac{dr}{r^2} \int_0^r \xi^2 \rho(\xi) d\xi \right\}^{1/2}, \quad (8)$$

in which $\eta = r_0/r$ and M_0 is the initial Mach number of the flow in the jet. The positive and negative choices for the value of the derivative $d\eta/d\varphi$ in eq.(8) have to be chosen with care. For example, if we consider the case in which no gravity and no pressure gradients are taken into account (i.e. the last two terms on the right hand side of eq.(8) are zero, which corresponds to a straight trajectory) the derivative $d\eta/d\varphi < 0$ for $\eta_* < 1/\sin \varphi_0$ and vice versa. The equality $\eta_* = 1/\sin \varphi_0$ corresponds to the point at which a given fluid element in the jet reaches the y axis during its motion in this particular case.

In the limit of high initial supersonic motion ($M_0 \gg 1$) the third and fourth terms on the right hand side of eq.(8) are important only when $\eta = 1/\sin \varphi_0$ and we can simplify eq.(8) by making an expansion about this point. In general terms, if:

$$\left(\frac{p}{p_0}\right)^\Gamma = \alpha + \beta\eta \sin \varphi_0 + \zeta\eta^2 \sin^2 \varphi_0, \quad (9)$$

and

$$\phi - \phi_0 = 4\pi G \left(\tilde{\alpha} + \tilde{\beta}\eta \sin \varphi_0 + \tilde{\zeta}\eta^2 \sin^2 \varphi_0 \right) \quad (10)$$

are expansions of the pressure and gravitational potential respectively around $\eta = 1/\sin \varphi_0$, then eq.(8) takes the form:

$$\frac{d\eta}{d\varphi} = \pm \frac{1}{\sin \varphi_0} \{a + b\eta + e\eta^2\}^{1/2}, \quad (11)$$

in which:

$$\begin{aligned} a &\equiv 1 - \frac{2(\alpha - 1)}{\gamma\Gamma M_0^2} - \frac{8\pi G}{M_0^2 c_0^2} \tilde{\alpha}, \\ b &\equiv - \left(\frac{2\beta}{\gamma\Gamma M_0^2} + \frac{8\pi G}{M_0^2 c_0^2} \tilde{\beta} \right) \sin \varphi_0, \\ e &\equiv - \left(1 + \frac{2\zeta}{\gamma\Gamma M_0^2} + \frac{8\pi G}{M_0^2 c_0^2} \tilde{\zeta} \right) \sin^2 \varphi_0, \end{aligned}$$

to second order in $\eta \sin \varphi_0$. For the cases considered in this analysis, the general solution of eq.(11) is:

$$\eta = \frac{1}{2e} \left\{ \sqrt{\Delta} \sin \left[\sqrt{-e} \left(\frac{\varphi_0 - \varphi}{\sin \varphi_0} + \frac{1}{\sqrt{-e}} \arcsin \frac{2e + b}{\sqrt{\Delta}} \right) \right] - b \right\} \quad (12)$$

with $\Delta \equiv b^2 - 4ae$. The angle between the velocity vector of the jet streamline and the x coordinate axis on its way out of the cloud (deflection angle) can be calculated from the relation $\tan \psi = (v_y/v_x)_{\text{exit}}$, in other words,

$$\psi = \arctan \left(\frac{\sin \varphi_e (d\eta/d\varphi)_e - \cos \varphi_e}{\cos \varphi_e (d\eta/d\varphi)_e + \sin \varphi_e} \right) + \pi, \quad (13)$$

where the exit azimuthal angle φ_e is given by:

$$\varphi_e = \varphi_0 + \frac{\sin \varphi_0}{\sqrt{-e}} \left\{ 2 \arcsin \frac{2e + b}{\sqrt{\Delta}} + \pi \right\}, \quad (14)$$

provided the deflections are not large. The derivative $(d\eta/d\varphi)_e$ is evaluated at $\eta = 1$, with a negative choice of sign in eq.(8).

3.1 Isothermal Cloud

Let us consider the case of an isothermal cloud, for which the density in the cloud $\rho_{\text{cloud}} = \xi/r^2$. In other words, because the jet and cloud are maintained in pressure balance, the pressure on the jet is given by:

$$\frac{p}{p_0} = \left(\frac{r_0}{r} \right)^2. \quad (15)$$

For this isothermal case, it is easy to verify that:

$$\begin{aligned} \alpha &= \frac{1 - \Gamma(3 - 2\Gamma)}{\sin^{2\Gamma} \varphi_0}, & \tilde{\alpha} &= \xi \ln(\sin \varphi_0) + \frac{3}{2}\xi, \\ \beta &= \frac{4\Gamma(1 - \Gamma)}{\sin^{2\Gamma} \varphi_0}, & \tilde{\beta} &= 2\xi, \end{aligned} \quad (16)$$

$$\zeta = \frac{\Gamma(2\Gamma - 1)}{\sin^{2\Gamma} \varphi_0}, \quad \tilde{\zeta} = \frac{\xi}{2}. \quad (17)$$

This solution corresponds to that found by Raga & Cantó (1996) for the case in which no gravity is present, i.e. $\tilde{\alpha} = \tilde{\beta} = \tilde{\zeta} = 0$. From the solutions obtained above in eq.(11) and eq.(16) it follows that the dimensionless quantity $\Lambda \equiv G\xi/M_0^2 c_0^2$ is a number that parametrises the required solution.

The deflection of jets in isothermal clouds may be important for interstellar molecular clouds and the jets associated with Herbig-Haro objects. For this case we can obtain a value for the parameter Λ . If we adopt a particle number density of $n_H \sim 10^2 \text{ cm}^{-3}$, and a temperature $T \sim 10 \text{ K}$ for a cloud with radius $r_0 \sim 1 \text{ pc}$ (Spitzer 1998; Hartmann 1998), then

$$\Lambda \sim \frac{10^{-2}}{M_0^2} \left(\frac{r_0}{1 \text{ pc}} \right)^2 \left(\frac{n_0}{10^2 \text{ cm}^{-3}} \right) \left(\frac{T}{10 \text{ K}} \right)^{-1}. \quad (18)$$

The same calculation can be made for the cases of radio jets interacting with the gas inside a cluster of galaxies. For this case, typical values are $n_H \sim 10^{-2} \text{ cm}^{-3}$, $T \sim 10^7 \text{ K}$ and $r_0 \sim 100 \text{ kpc}$ (Longair 1992; Longair 1998). With these values, the parameter $\Lambda \sim 10^{-2}/M_0^2$, exactly as eq.(18). The parameter Λ is an important number which can be obtained by dimensional analysis. For, the problem in question is characterised by the gravitational constant G , a ‘‘characteristic length’’ r_0 and the values of the velocity of the jet and the density v_0 and ρ_0 respectively. Three independent dimensions (length, time and mass) describe the whole hydrodynamical problem. Since four independent physical quantities (G , ρ_0 , v_0 , and r_0) are fundamental for the problem we are interested, the Buckingham II–Theorem of dimensional analysis requires the existence of only one dimensionless parameter $\Lambda = G\xi/M_0^2 c_0^2$, exactly as in the analytic solution. The fact that jets are formed in various environments such as giant molecular clouds and the gaseous haloes of clusters of galaxies with the same values of the dimensionless parameter Λ provides a clue as to why the jets look the same in such widely different environments.

From its definition, the parameter Λ can be rewritten as $\Lambda = (3/4\pi)(GM/r)(1/v_0^2)$, where M is the mass within a sphere of radius r_0 . This quantity is roughly the ratio of the gravitational potential energy from the cloud acting on a fluid element of the jet, to its kinetic energy at the initial position r_0 . The parameter Λ is thus an indicator of how large the deflections due to gravity are going to affect the trajectory of the jet. The bigger the number Λ , the more important the deflection caused by gravity will be. In other words, when the parameter $\Lambda \gg 1$ the jet becomes ballistic and bends towards the centre of the cloud. When $\Lambda \ll 1$ the deflections are dominated by the pressure gradients in the cloud and the jets bend away from the centre of the cloud.

Fig.(1) shows plots for three different values of Λ with

initial Mach numbers of $M_0 = 5$ and $M_0 = 10$. A comparison with a numerical integration of eq.(11) using a fourth-order Runge–Kuta method is also presented in the figures by dashed lines. This comparison shows that as long as the deflections are sufficiently small, or as long as the Mach number of the flow in the jet is sufficiently large, the analytic approximations discussed above are a good approximation to the exact solution.

3.2 Gas on Dark Matter Halo

Let us consider next the case of a galaxy dominated by a dark matter halo for which the mass density is given by the relation (Binney & Tremaine 1987):

$$\rho_d = \frac{\rho_{d_*}}{1 + \left(\frac{r}{a}\right)^2}, \quad (19)$$

in which a is the core radius and quantities with a star refer to the value at the centre of the galaxy.

The potential resulting from such a density profile can be calculated by means of eq.(7),

$$\phi_d - \phi_{d_*} = 4\pi G \rho_{d_*} a^2 \times \left\{ \frac{1}{2} \ln \left[1 + \left(\frac{r}{a}\right)^2 \right] + \frac{a}{r} \arctan \left(\frac{r}{a}\right) - 1 \right\}, \quad (20)$$

in which the value of the gravitational potential ϕ_{d_*} has been evaluated at the centre of the galaxy $r_* = 0$. If the gas in the galaxy is in hydrostatic equilibrium with the dark matter halo, then $\mathbf{grad} p = -\rho \mathbf{grad} \phi_d$. In this case, the enthalpy of the isothermal gas is given by:

$$w - w_* = -\phi_d + \phi_{d_*} = c_*^2 \ln \left(\frac{p}{p_*}\right), \quad (21)$$

and so the pressure is:

$$p = p_* \exp \left\{ (-\phi_d + \phi_{d_*}) / c_*^2 \right\}. \quad (22)$$

It is possible to simplify the above expressions using the fact that for astronomical cases $r_0 \gg a$. In other words:

$$\frac{p}{p_0} = \eta^{-k}, \quad (23)$$

where $k = -4\pi G \rho_{d_*} a^2 / c_*^2$. In this approximation, the required analytic solutions can be found:

$$\begin{aligned} \alpha &= \frac{1}{2} (\Gamma k + 1) (\Gamma k + 2) \sin^{\Gamma k} \varphi_0, \\ \beta &= -\Gamma k (2 + \Gamma k) \sin^{\Gamma k} \varphi_0, \\ \zeta &= \frac{1}{2} \Gamma k (\Gamma k + 1) \sin^{\Gamma k} \varphi_0, \end{aligned} \quad (24)$$

where for simplicity it was assumed that $\tilde{\alpha} = \tilde{\beta} = \tilde{\zeta} = 0$, in other words we neglect the gravitational field induced by the mass of the cloud. Typical values (Binney & Tremaine 1987) for galaxies are $\rho_* \sim 0.1 M_\odot \text{pc}^{-3}$, $a \sim 1 \text{kpc}$. Taking central values for the gas in the galaxy as $n_* \sim 1 \text{cm}^{-3}$ and $T_* \sim 10^5 \text{K}$ then $k \sim -10$. Fig.(2) presents plots for different values of M_0 and k .

The dimensionless number k which parametrises the required solution can be obtained by dimensional analysis (apart from an unimportant factor of -4π) in the same way as the parameter Λ was obtained in Section 3.1. In this case the important parameters in the problem are the gravitational constant G , the characteristic length a and the sound speed c_* . The number k can be rewritten as $k = -(4/(4 - \pi)) (GM/a)(1/c_*^2)$, where M is the mass of a sphere with radius a . This quantity is proportional to the gravitational energy of the cloud evaluated at the core radius divided by the sonic kinetic energy that a fluid element in the jet has. In other words, in the same way as in Section 3.1, the dimensionless number k is an indicator as to how big deflections produced by gravity are.

4 RELATIVISTIC ANALYSIS

Let us consider the case in which relativistic effects are included in the interaction of a relativistic jet and a stratified high density region. In order to simplify the problem, the self gravity of the cloud acting on the jet is ignored. For this case, the relativistic 4-Euler's equation is:

$$w u^k \frac{\partial u_i}{\partial x^k} = \frac{\partial p}{\partial x^i} - u_i u^k \frac{\partial p}{\partial x^k} \quad (25)$$

in which w , and p are the enthalpy per unit volume and the pressure of a given fluid element in its proper frame of reference respectively (Landau & Lifshitz 1987). The 4-velocity $u^k = dx^k/ds$ (latin indices run as 0, 1, 2, 3) is given by $(\gamma, \gamma \mathbf{v}/c)$, c is the speed of light and γ is the Lorentz factor. The 4-radius vector $x^k = (ct, \mathbf{r})$ and the metric tensor $\eta_{kl} = \text{diag}(1, -1, -1, -1)$. The space component of eq.(25) can be written as:

$$\frac{w \gamma^2}{c^2} \left(\frac{\partial \mathbf{v}}{\partial t} + \mathbf{v} \cdot \mathbf{grad} \mathbf{v} \right) = -\mathbf{grad} p - \frac{\mathbf{v}}{c^2} \frac{\partial p}{\partial t}, \quad (26)$$

which is the generalisation of Euler's equation. As before, the term in brackets on the left-hand side represents the classical force per unit mass acting on an element of fluid as it moves. By considering steady flow and noting that all quantities depend only on the radial coordinate r , vector multiplication of the radius vector \mathbf{r} with eq.(26) shows that the quantity $\mathbf{l} = \mathbf{r} \times \mathbf{v}$ is conserved as the fluid moves. This quantity corresponds to the classical equivalent of the specific angular momentum, but it is not the relativistic angular momentum which is given by $\mathbf{r} \times \gamma \mathbf{v}$. The constancy of \mathbf{l} shows that the motion is two dimensional and so eqs.(2)-(3) are valid in the relativistic case as well.

The trajectory of the jet is described by Bernoulli's equation, which is given by the time component of eq.(25) for steady adiabatic flow by (Landau & Lifshitz 1987):

$$\int d \left(\frac{\gamma w}{n} \right) = 0. \quad (27)$$

The line integral is taken from the initial position of a given fluid element to its final one. The particle number per unit proper volume is n and we assume that the electrons in the jet are ultrarelativistic, so that the equation of state is given by $p = e/3$ with e being the internal energy density

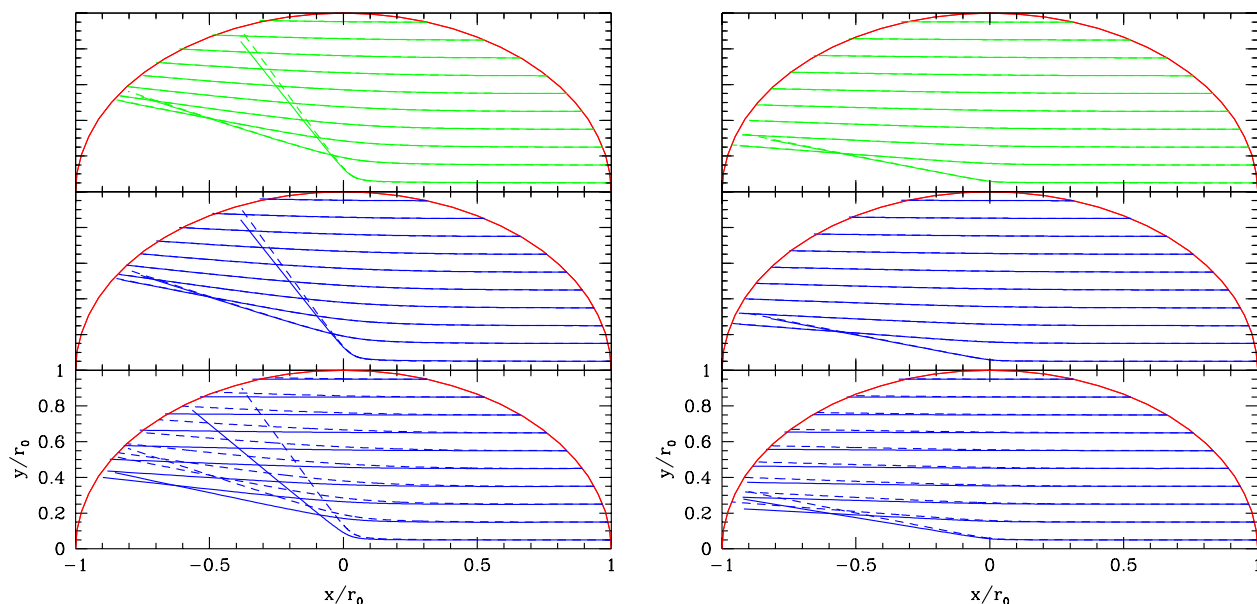


Figure 1. Deflection produced in a jet due to the interaction with an isothermal cloud (semicircle) of radius r_0 . The jet penetrates the cloud from the right, parallel to the x axis. Different trajectories are shown in each diagram for different initial heights of $y/r_0 = 0.05, 0.15, \dots, 0.95$ as measured from the x/r_0 axis. In each figure the top diagram corresponds to the case in which gravitational effects are not considered (Raga & Cantó 1996). The central and bottom diagrams represent trajectories for which gravitational effects are taken into account and the parameter Λ has values of 10^{-6} , and 0.01 respectively in units of the square of the initial Mach number M_0^2 of the jet (see text). A polytropic index $\gamma = 5/3$ for the flow in the jet was assumed. The diagrams at the left and right correspond to initial Mach numbers for the jet flow of $M_0 = 5$ and $M_0 = 10$ respectively. The dashed lines in the graphs represent the direct numerical integration of the equation of motion. The continuous lines are the analytic approximations discussed in this article.

of the fluid. The requirement that the pressure of the jet equals that of the cloud, together with the fact that $p \propto n^{4/3}$ gives:

$$\frac{d\eta}{d\varphi} = \pm \frac{c}{v_0 \sin \varphi_0} \left\{ 1 - \frac{v_0^2}{c^2} \eta^2 \sin^2 \varphi_0 - \gamma_0^{-2} \left(\frac{p}{p_0} \right)^{1/2} \right\}^{1/2}, \quad (28)$$

in which $\eta \equiv r_0/r$. The sign of $d\eta/d\varphi$ in eq.(28) varies as the jet crosses the cloud. For example, for the ultrarelativistic case, in which a straight trajectory is expected, it is positive for $\eta_* > 1/\sin \varphi_0$, and negative when the inequality is inverted. A general analytic solution of eq.(28) can be found by noting that for high relativistic velocities the third term on the right hand side of eq.(28) is important only for $\eta = 1/\sin \varphi_0$. In other words, the pressure stratification of the cloud can be written as eq.(9) with $\Gamma \rightarrow 1/2$. We can therefore expand eq.(28) around $\eta = 1/\sin \varphi_0$ to obtain a relation which is the same as eq.(11) but with:

$$a = 1 - \frac{\alpha}{\gamma_0^2}, \quad b = -\frac{\beta}{\gamma_0^2} \sin \varphi_0, \quad e = -\left(\frac{\zeta}{\gamma^2} + 1 \right) \sin^2 \varphi_0. \quad (29)$$

4.1 Isothermal Cloud

As in section 3.1, consider the case in which the jet propagates through an isothermal cloud. In this case it is possible

to find an exact solution to the problem, since eq.(15) and eq.(28) imply:

$$\frac{d\eta}{d\varphi} = \pm \frac{1}{\sin \varphi_0} \left\{ \frac{c^2}{v_0^2} (1 - \eta \gamma_0^{-2}) - \eta^2 \sin^2 \varphi_0 \right\}^{1/2}. \quad (30)$$

In other words, the solution is the same as the one already found in eq.(11) and eq.(12) but with:

$$a = \left(\frac{c}{v_0} \right)^2, \quad b = -\left(\frac{c}{v_0} \right)^2 \gamma^{-2}, \quad e = -\sin^2 \varphi_0. \quad (31)$$

Fig.(3) shows plots of the trajectory of the jet for different values of the initial velocity of the jet.

4.2 Gas on a Dark Matter Halo

As in section 3.2 for $r_0 \gg a$, the variation of the pressure in the galaxy is given by eq.(23) and the trajectory of the path of the jet is given by eq.(11) and eq.(12) together with eq.(24) and the substitution $\Gamma \rightarrow 1/2$. Fig.(4) shows plots of this for $k = -3$ and different values of the initial velocity of the jet v_0 .

5 DISCUSSION

When a deflection is observed, it is possible to work backwards and find useful properties concerning the initial interaction of a jet with a stratified density region. For example,

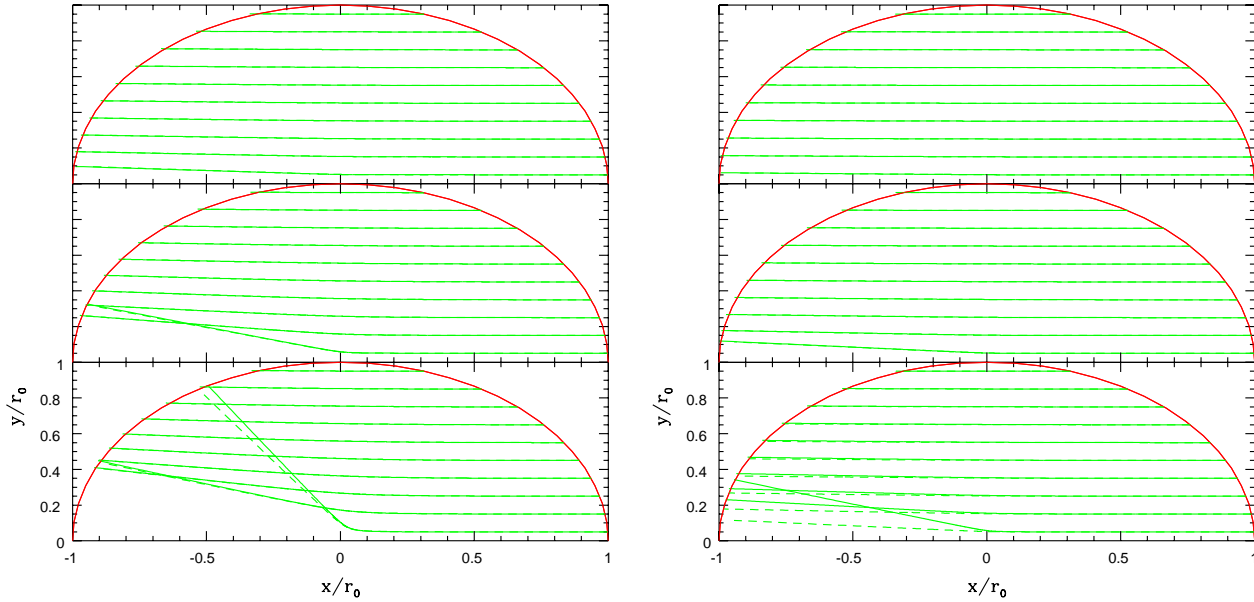


Figure 2. Deflection produced in a jet as it travels across a galaxy, for which its gravitational potential is dominated by a dark matter halo. The jet penetrates the galaxy parallel to the x/r_0 axis. Various trajectories are shown in each diagram for different initial heights $y/r_0 = 0.5, 0.15, \dots, 0.95$ measured from the x/r_0 axis. The left and right diagrams were calculated for the case of a non relativistic jet with an initial Mach number of $M_0 = 10$ and $M_0 = 20$ respectively. For each of this diagrams a value of $k = -1, -2, -3$ was used for the top, middle and bottom panels respectively (see text). The dashed lines in the figures represent the direct numerical integration of eq.(11) with the pressure given by eq.(22) for the case in which the ratio of the core radius a to the initial radius r_0 is given by $a/r_0 = 10^{-3} \ll 1$. The continuous lines are analytic approximations found under this conditions.

by taking the “standard” values used in sections 3.1 and 3.2 for the pressure and density in the stratified gas it is possible to calculate the initial azimuthal angle φ_0 for a given initial velocity of the jet. Indeed, from eq.(13) and eq.(14), together with the negative derivative $(d\eta/d\varphi)_e$ at the moment the jet leaves the cloud we can find the value of the deflection angle $\cos \psi$ as a function of the velocity of the jet v_0 and the initial azimuthal angle φ_0 . The curves for which $\cos \psi = \text{const}$ give the required relation between the initial velocity and azimuthal angle. Fig.(5) shows two examples of this type of analysis.

Different combinations of the various parameters involved (or the known observables) in the problem can be formed so that, for a given deflection, the other quantities can be calculated. For instance one can ask for the values of the central density of the gas in the cloud, the density in the jet, etc.

The assumption of pressure equilibrium between the jet and the external environment has certain limitations on the geometry of the jet (Raga & Cantó 1996). In the non-relativistic limit pressure equilibrium is achieved, when the time for a pressure scale height $(p(r)/|dp(r)/dr|)$ to change significantly within the jet material is greater than the sound crossing time of the jet radius:

$$\frac{\Delta_j}{c_j} \ll \frac{1}{v_j} \frac{p(r)}{|dp(r)/dr|}, \quad (32)$$

where c_j is the speed of sound in the jet, v_j its velocity and Δ_j its radius (Raga & Cantó 1996). For the case of an

isothermal sphere the right hand side of eq.(32) is $r/2v_j$ and for the case of gas in pressure equilibrium with a dark matter halo is $r/|k|v_j$. In the case of relativistic flow, eq.(32) is still valid but with the substitution $v_j \rightarrow \gamma_{v_j} v_j$ and $c_j \rightarrow \gamma_{c_j} c_j$, where γ_{v_j} and γ_{c_j} are the Lorentz factors of the flow velocity and the velocity of sound respectively.

When a jet bends it is in direct contact with its surroundings and entrainment from the external gas might cause disruption to its structure (Icke 1991). However, if this situation is bypassed for example, by an efficient cooling, then there remains a high Mach number collimated flow inside a curved jet. When supersonic flow bends, the characteristics emanating from it intersect at a certain point in space (Landau & Lifshitz 1987). Since the hydrodynamical values of the flow in a characteristic line have constant values, the intersection causes the different values of these quantities to be multivalued. This situation can not occur in nature and a shock wave is formed.

The formation of internal shocks inside the jet gives rise to subsonic flow inside the jet and collimation may no longer be achieved. If the characteristic lines produced by the flow inside the jet intersect outside the jet, then a shock wave is not formed and the jet remains collimated as it bends. However, two important points have to be considered in the discussion. The first is that the Mach number decreases in a bend as the flow moves. The second is that the rate of change of the Mach angle with respect to the angle the jet makes with its original straight trajectory (the bending angle) increases without bound as the velocity of the flow tends to that of the local velocity of sound. This was first proved

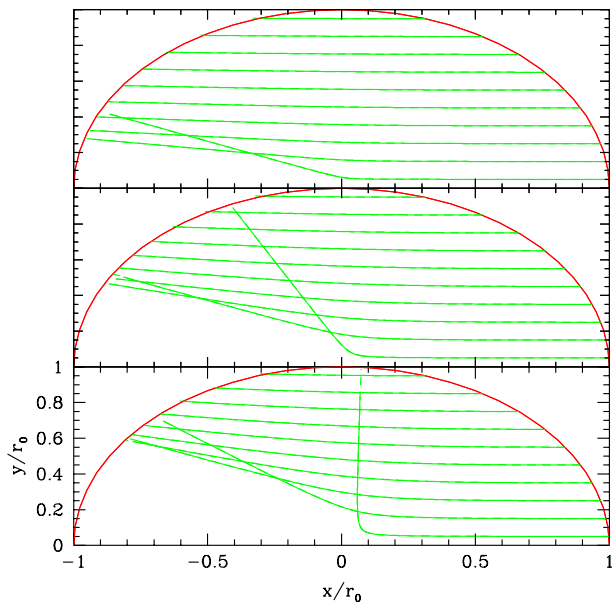


Figure 3. Deflection of a relativistic jet produced by its interaction with an isothermal cloud (semicircle). The jet is assumed to travel parallel to the x axis at the moment it enters the cloud from the right. In each plot different trajectories are shown for different values of the initial height of the jet $y/r_0 = 0.05, 0.15, \dots, 0.95$ as measured from the x/r_0 axis. The top, central and bottom panel plots were calculated for values of the initial velocity of the jet v_0 in units of the speed of light c of 0.99, 0.97, 0.95 respectively.

by Icke (1991) for the case in which no relativistic effects were taken into account. We have made a relativistic generalisation to these two points which will be discussed in a future paper. The increase in the Mach angle means that there has to be a stage at which this angle grows faster than the bending angle. This causes the characteristics in the jet to intersect and to form a shock. The only way to avoid this situation is if the rate of change of the Mach angle with respect to the bending angle is less than one. The formation of this shock is most probably not too destructive for the jet. This is because the Mach number of the flow is close one, which implies that the shock is weak.

The fact that two shocks might form inside a jet, one of them at the end of the bending when the Mach number is near one, enables us to find an upper limit to the bending angle (Icke 1991). For example, a classical jet with $\gamma = 5/3$ cannot be deflected more than 60.8° . Under the same classical conditions, but by assuming a polytropic index $\gamma = 4/3$, classical jets with a relativistic equation of state cannot be deflected more than 148.12° (Icke 1991).

When a full relativistic analysis is introduced in this description, this upper limit can not be greater than its classical counterpart. The relativistic Mach angle (Königl 1980) decreases as the velocity of the flow approaches that of light. This means that characteristic lines emanating from a relativistic flow are closer to the streamlines as compared with their classical counterparts. The fact that characteristic lines are closer to the streamlines means that when a bending occurs, the chance for an intersection between different

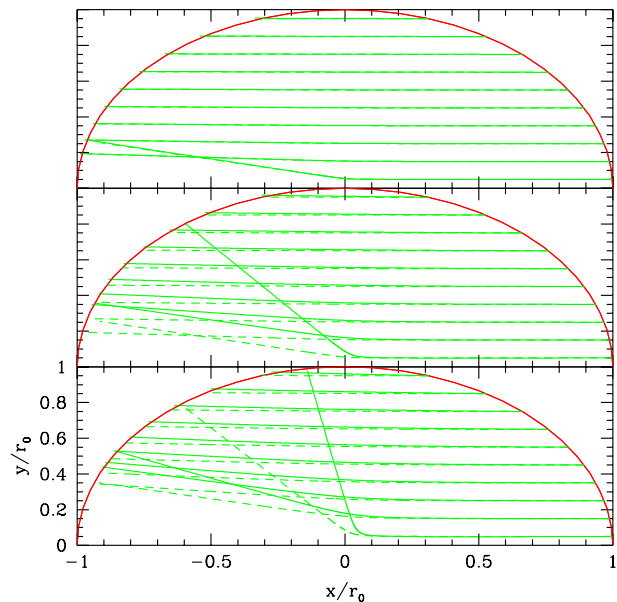


Figure 4. Trajectory of a jet as it crosses a galaxy. The gas in the galaxy is assumed to be in hydrostatic equilibrium with a gravitational potential given by a dark matter halo in the galaxy. It is assumed that the jet enters the galaxy parallel to the x axis at a height of $y/r_0 = 0.05, 0.15, \dots, 0.95$ in different cases. The plots were calculated for the case in which the parameter $k = -3$ and the initial velocity of the jet in units of the speed of light is 0.999, 0.995 and 0.99 from top to bottom. Continuous lines are analytic approximations for a high Mach number of the flow inside the jet. The dashed lines are direct numerical solutions.

characteristics increases. As a result, a relativistic jet with a polytropic index $\gamma = 4/3$ can not bend more than 47.94° . The precise conditions under which an internal shock is produced for a given jet depend on the shape of the curve that the jet makes as it bends and the radius of the jet. The general conclusion is that, provided the jets are sufficiently narrow, the deflections shown in figs.(1)-(4) are valid for small deflections, say $\lesssim 20\text{--}30^\circ$.

As an example, we can take the case of the western jet in the radio galaxy 3C34 (Best, Longair & Röttgering 1997). If this jet was bent because of the interaction with a typical galaxy for which its gas is in pressure equilibrium with a dark matter halo, then we can use the standard values presented in section 4.2. First of all, the western jet in 3C34 has a bending angle $\Theta \sim 10^\circ$, so that the deflection angle $\psi \sim 170^\circ$. If we assume that the flow inside the jet moves with a velocity $v = 0.99c$, it follows from the right diagram in fig.(5) that $\sin \varphi_0 \sim 0.3$, or $\varphi_0 \sim 17^\circ$. On the other hand, the value $\Theta \sim 10^\circ$ is well below the upper limit of 47.94° discussed above, so that at least no terminal shock will be produced by the deflection of the jet. From preliminary results that will be published elsewhere, it follows that if the trajectory of the jet in 3C34 is circular, then in order not to produce an internal shock at the onset of the curvature, the ratio D/R (D is the width of the jet and R its radius of curvature) has to be less 0.08. In other words, the destruction of jets only occurs if the jets are thick, rather than narrow. This result

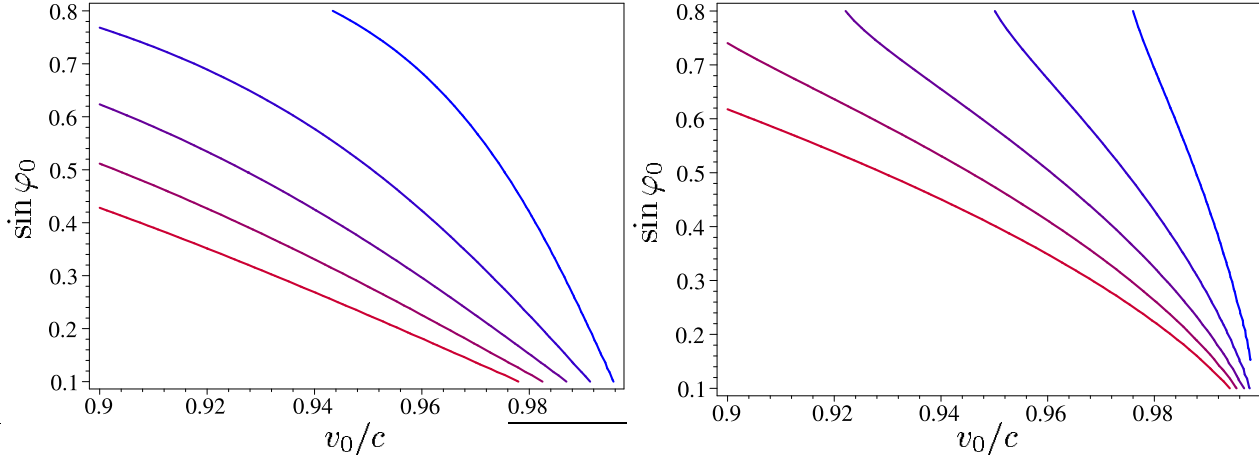


Figure 5. Variations of initial azimuthal angle φ_0 as a function of velocity v_0 in units of the speed of light c for constant values of the deflection angle ψ . The angle ψ is the azimuthal angle the velocity vector of the flow in the jet makes with the x axis at the moment it leaves the cloud. Every plot was calculated for $\cos \psi = \text{const}$ with values given by ψ of $175^\circ, 170^\circ, \dots, 155^\circ$. The gradient of ψ decreases towards the lower left part of each diagram. In other words, deflections become stronger as the curves approach this region on the diagram. An isothermal sphere and an isothermal gas in hydrostatic equilibrium with a dark matter halo were assumed for the left and right diagrams respectively in the case of a relativistic jet.

is in accord with the narrowing of jets observed in a wide range of different sources.

The most important consequence of the calculations presented in this article is the sensitivity of the deflection angles to variations in velocity (see for example fig.(5)). This sensitivity is due to the fact that the force applied to a given fluid element in the jet (due to pressure and gravitational potential gradients) is the same independent of the velocity of the flow in the jet. However, as the velocity of the flow in the jet increases, there is not enough time for this force to change the curvature of the jet soon enough, giving rise to very straight jets.

6 ACKNOWLEDGEMENTS

We would like to thank P. Scheuer for useful comments during the preparation of this article. S. Mendoza thanks support granted by Dirección General de Asuntos del Personal Académico (DGAPA) at the Universidad Nacional Autónoma de México (UNAM).

REFERENCES

- Begelman M.C., Blandford R.D., Rees M.J., 1984, *Rev. Mod. Phys.* 56, 255
 Binney J., Tremaine S., 1987, *Galactic Dynamics*, Princeton University Press
 Blandford R.D., 1990, in *Active Galactic Nuclei*, Saas-Fee Advanced Course 20, Les Diablerets, Springer-Verlag
 Best P.N., Longair M.S., Röttgering H.J.A., 1997, *MNRAS* 286, 785B
 Best P.N., Carilli C.L., Garrington, S.T., Röttgering, H.J.A., Longair M.S., 1998, *astro-ph/9803130*
 Best, P. N., Röttgering, H. J. A. and Longair, M. S. 2000, *MNRAS*, 311, 23
 Cantó J., Raga A.C., 1996, *MNRAS*, 280, 559
 Hartmann L., 1998, *Accretion Processes in Star Formation*, CUP

- Icke V., 1991, in *Beams and Jets in Astrophysics*, CUP
 Königl A., 1980, *Physics of Fluids*, 23, 1083
 Landau L.D., Lifshitz, E.M., 1987, *Fluid Mechanics*, Pergamon
 Longair M.S., 1992, *High Energy Astrophysics*, CUP
 Longair M.S., 1998, *Galaxy Formation*, Springer
 Raga A.C., Cantó J., 1995, *Rev. Mex. Astron. Astrofis.*, 31, 51
 Raga A.C., Cantó J., 1996, *MNRAS*, 280, 567
 Spitzer L., 1998, *Physical Processes in the Interstellar Medium*, Willey